Theoretical study of benzene and pyridine STM-induced reactions on copper surfaces

2008 J. Phys.: Condens. Matter 20 224012

(http://iopscience.iop.org/0953-8984/20/22/224012)

J. Phys.: Condens. Matter **20** (2008) 224012 (7pp) doi:10.1088/0953-8984/20/22/224012

Theoretical study of benzene and pyridine STM-induced reactions on copper surfaces

H Lesnard[1], N Lorente[2] and M-L Bocquet[1]

[1] Laboratoire de Chimie, UMR 5182, ENS Lyon, 69364 Lyon Cédex 07, France
[2] Centro de Investigaciones en Nanociencia y Nanotecnología, CSIC, Campus de la Universidad Autónoma de Barcelona, 08193 Bellaterra, Spain

E-mail: hlesnard@ens-lyon.fr, lorente@icmab.es and mbocquet@ens-lyon.fr

Received 8 November 2007
Published 13 May 2008
Online at stacks.iop.org/JPhysCM/20/224012

Abstract

Density functional theory calculations are used to determine the adiabatic reaction pathways of STM-induced reactions of benzene and pyridine molecules on Cu(100), Cu(110) and Cu(111). The studied reactions are rupture of the molecular ring as well as dehydrogenation of the molecules. In order to establish the final fragments of the reactions, the inelastic electron tunneling spectra of the molecules are analyzed and rationalized in terms of the electronic structure of the system. Besides vibrational excitation, the impinging electron confers on the molecule a dynamical evolution that depends on the capacity of the system to damp the excess energy. We predict that in the limit of heavy fragments, and hence for the heaviest isotopes, the STM bias voltage will match the computed adiabatic barriers.

(Some figures in this article are in colour only in the electronic version)

1. Introduction

Inelastic effects in tunneling currents can be used to induce chemical reactions on the molecular scale [1–4]. These effects are also at the origin of a recent measuring mode of the STM [5]. Indeed, inelastic electron tunneling spectroscopy (IETS) with the STM has proved to be a unique chemical probe in determining molecular species and conformations on surfaces [5–8]. Combined with density functional theory (DFT) based calculations, the experimental changes in conductance giving rise to IETS can be accurately interpreted [9–12]. Recently, the identification of the dehydrogenation product of benzene after an STM pulse has been made possible by IETS simulations [12]. Yet, the analysis of the products alone is not sufficient to characterize the reaction and there is a lot of activity devoted to the evaluation of the actual reaction pathways. The theoretical state of the art is quickly evolving and DFT has now reached the level of quantitative predictions of reaction barriers [13].

Recently, we have applied these techniques to the analysis and understanding of benzene and pyridine dehydrogenation under an STM pulse [14] motivated by the experimental work of [15, 16]. In the present contribution, we extend these results to the study of the molecular-ring rupture of benzene and pyridine, as well as dehydrogenation over the Cu(100), Cu(110) and Cu(111) surfaces. Due to the importance of IETS measurements, we analyze the absence of IETS signal in the C–H stretch modes of chemisorbed benzene in terms of its electronic structure. We also analyze the case of pyridine and its dehydrogenation fragment. However, the electronic structure is not enough to understand the reaction processes. We finalize the paper by discussing the role of non-adiabatic effects and how in the limit of large masses our computed energy barriers should be retrieved, hence permitting us to predict an isotopic dependence of the bias voltage.

2. Method

The VASP code [17] has been used to determine the electronic, vibrational and energetic properties of the molecule–surface system. The electron–ion interaction is described by the projector-augmented wave (PAW) scheme in the VASP implementation [17, 18] and the electronic wavefunctions are expanded by plane waves up to a kinetic energy of 400 eV. The Cu(111) and Cu(100) surfaces are modeled with four atomic layers of copper plus the adsorbed molecule and a vacuum region of some 15 Å. The more open Cu(110) surface was approximated by a six-layer slab. The calculations are performed with the theoretical Cu lattice constant of

3.65 Å using a p(4 × 4) surface periodicity. We use a *k*-point set with 16 points in the surface Brillouin zone. The uppermost two copper layers as well as the molecular degrees of freedom are allowed to relax until atomic forces are lower than 0.01 eV $Å^{-1}$.

The adiabatic reaction barriers were obtained by finding the saddle points of the potential energy surface (PES) connecting the phase spaces of reactant and product. These saddle points define the moment when the system departs from a given structure to become something else; they are thus the transition states (TSs) of the reaction pathway. Approximate structures of TSs are obtained with the minimization of a set of eight intermediate images using the nudged elastic band method [19]. To refine the TS geometry we have further minimized all the residual forces with a quasi-Newton algorithm. Finally, the TS is identified by exhibiting the existence of a single normal mode associated with a pure imaginary frequency; an imaginary frequency means that the PES has turned from concave to convex, revealing the appearance of a saddle point and, hence, of a TS. The larger the modulus of the imaginary frequency, the steeper the descent along the reaction coordinates.

The modes of the stable relaxed structures are evaluated by diagonalization of the dynamical matrix. This matrix is obtained by a finite-difference method implemented in VASP. In this vibrational analysis, only the degrees of freedom of the relaxed adsorbate are considered (molecular vibrations) because we are interested in IETS signals of high frequency (C–H stretch frequencies) that are little perturbed by the low-frequency modes originating from surface phonons. The IETS simulations are performed with a many-body extension of the Tersoff–Hamman theory [20] used for the STM [9, 11, 12] simulations.

The results of this work are rationalized in terms of energy barriers and the combined molecule–substrate electronic structure. In order to analyze the full electronic structure, we use the molecular orbitals (MOs) of the molecular fragment of interest. Thus, by retaining the percentage of MO character of a given eigenstate of the full system, we analyze the electronic structure in terms of its molecular character. This is finally presented in the form of a weighted density of states named the projected density of states (PDOS) onto molecular orbitals given by the expression

$$\mathrm{PDOS}(E) = \sum_{\lambda} |\langle \mathrm{MO}|\lambda\rangle|^2 \delta(\epsilon_\lambda - E) \qquad (1)$$

where λ are the labels of the eigenenergies, ϵ_λ, and eigenstates, $|\lambda\rangle$, of the chemisorbed system and MO is the free-molecule state onto which the density of states is projected. The MO is calculated for the free molecular fragment in its chemisorption geometry.

3. Results

We have extended and completed the studies presented in [12, 14] to explore the effect of different substrates. Hence, we have evaluated the chemisorption properties of benzene on Cu(100), Cu(110) and Cu(111); we find that benzene is weakly adsorbed over the highest coordinated site on Cu(100) at a bonding distance of 2.3 Å and a chemisorption energy of 0.3 eV [14]. The more open surface, Cu(110), chemisorbs the molecule with its center between the short bridge (along direction $\langle 0\bar{1}1\rangle$) and the hollow sites. This leads to a tilted configuration that departs from the typical benzene flat adsorption geometry on metallic surfaces. This result is in agreement with cluster calculations [21, 22], that show that this surface is more active in the binding of benzene. Our calculated energy is 0.07 eV higher than for the (100) surface. The more packed (111) surface leads to a flat chemisorption on the hollow site, with a chemisorption energy 0.1 eV lower than the (100) surface. These trends follow the experimental behavior. Indeed, the adsorption data are available on Cu(111) [23, 24] and on Cu(110) [25]. On Cu(111) the adsorption energy estimated from a 225 K desorption temperature is 0.429 eV [23], while on Cu(110) the desorption temperature is rather 280 K [25].

Despite the similarities of benzene chemisorption on the three main Cu surfaces, we find that Cu(110) leads to a distorted molecular ring, and to considerable charge transfer. This signals that reactions induced on Cu(110) [16] may not be directly comparable with the same reactions performed on the two other more packed surfaces.

The adiabatic reaction pathways are evaluated using static calculations where the degrees of freedom of molecules and substrates are allowed to relax without taking the system out of the considered configuration. Thus they are static calculations that assume that the reaction is taking place without dissipation or non-adiabatic effects.

3.1. Benzene reactions

The STM-induced reactions are performed by ramping up the tip–molecule bias voltage. The experimental analyses [15, 16] conclude that benzene is dehydrogenated. We have shown before that good agreement with the experimental IETS is obtained if the fragment is phenyl (C_6H_5), the singly dehydrogenated fragment of benzene [12]. However, other fragmentation reactions may be possible.

The first reaction that we consider on the Cu(100) surface is the rupture of the benzene ring. As we have found before [26], there is some charge transfer into the π^* complex of the chemisorbed benzene molecule, leading to some weakening of the C–C ring. Hence, it might be possible to break the benzene ring. Figure 1(a) shows the lowest-energy ring dissociation path of benzene on Cu(100). We find that the transition state (TS) is very close to the reaction product, and hence we have only plotted the final state as TS in figure 1(a). In this case, the true TS is in between the very close initial and final products; the small distance in reaction space between these two products renders the true-barrier determination very difficult. We find that the energy difference between the initial and final products is 2.2 eV, already larger than the barrier for dehydrogenation. The actual barrier will be even larger, hinting that thanks to the C–C ring weakening due to chemisorption the actual rupture may be induced by the STM at typical operating conditions for molecular manipulation.

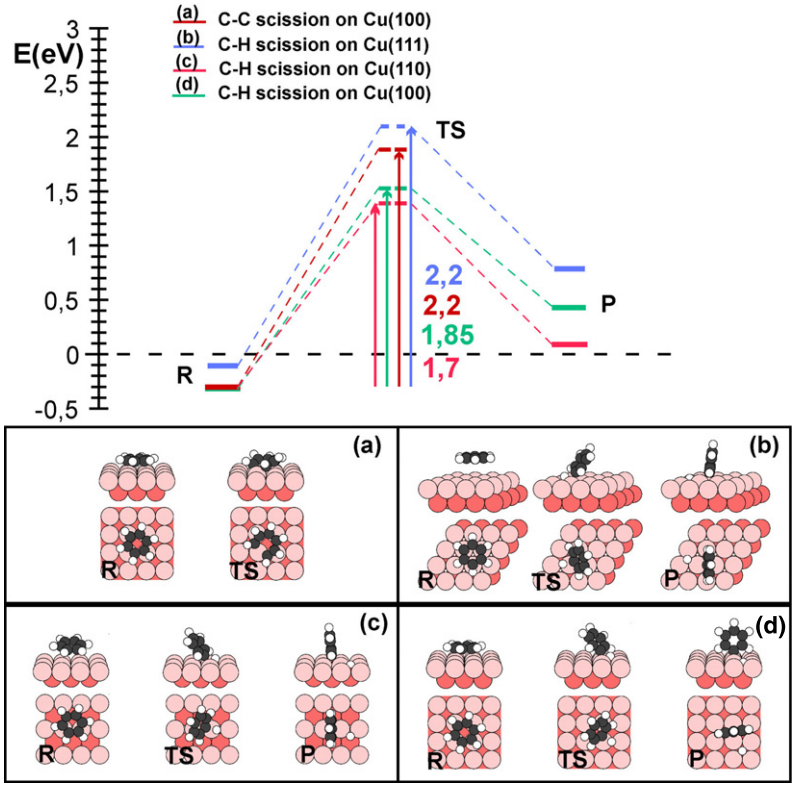

Figure 1. Adiabatic barriers for the reactions depicted in the lower panels: (a) C–C rupture of the benzene ring on Cu(100), (b) benzene dehydrogenation on Cu(111), (c) benzene dehydrogenation on Cu(110) and (d) benzene dehydrogenation on Cu(100).

The dehydrogenation process on Cu(111) (figure 1(b)), Cu(110) (figure 1(c)) and Cu(100) (figure 1(d)) is activated first by the partial desorption of the molecule. Indeed, the molecule ring separates from the surface and keeps its interaction with the surface mediated by a H atom. The H atom is attracted towards a bridge site due to the higher affinity of the bridge sites for H atoms as compared with the top site. This leads to a consequent elongation of the corresponding C–H bond, and its final rupture. The final state is a phenyl (C_6H_5) fragment chemisorbed on a bridge site in a di-sigma configuration. The H atom minimizes the total energy by chemisorbing on the highest coordinated site for each surface, as seen in figure 1. In all of the cases, the final products have a configuration of high energy as compared with the initially adsorbed benzene molecule. The TS lies at considerably higher energy, leading to barriers of 2.2 eV for Cu(111), 1.7 eV for Cu(110) and 1.85 eV for Cu(100).

The barrier trend with surface type can be rationalized in terms of the molecule–surface interaction. Indeed, the chemisorption energy is the weakest for the surface that has the largest dehydrogenation barrier: the Cu(111) surface. The chemisorption energy is consequently the largest for the surface with the lowest dehydrogenation barrier, namely Cu(110). The molecule–surface interaction is largely mediated by charge transfer from the substrate [26], leading to some slight population of antibonding molecular orbitals and hence to weakening of the internal molecular bonds as the molecule is more strongly attached to the surface. These results show that the presence of the surface has an enormous influence on the C–H dissociation barrier, such that small variations in the surface (such as going from the (111) to the (100) surface) lead to sizable barrier changes. Further analyses of the dehydrogenation barrier in the case of benzene on Cu(100) can be found in [14].

3.1.1. IETS of the reaction products. The experimental identification of the reaction products was performed by analyzing the IETS of the final fragments [15, 16]. The most striking finding was that except for benzene the fragments showed changes in conductance that agreed with the excitation of some C–H stretch mode or modes. Careful comparison of the experimental spectra with simulated IETS for phenyl and benzyne (C_6H_4) permitted us to determine that the final dehydrogenation product was phenyl [12]. In the present article, in addition to the IETS of phenyl we analyze the C–H stretch spectra of benzene and we rationalize the absence of IETS for these modes.

Figure 2(a) shows the change in conductance over the chemisorbed benzene molecule on Cu(100) for each C–H stretch mode. The maximum change in conductance for each mode is given in the corresponding panel. We find a maximum change in conductance of 0.3%, and the addition of all the modes leads to a change in conductance of 0.6%. In comparison, figure 2(b) shows the change in conductance for the phenyl fragment. The addition of the C–H stretch mode signals leads to an associated change in conductance of 8.1%, more than an order of magnitude larger than the corresponding change in conductance for benzene. Please notice that for

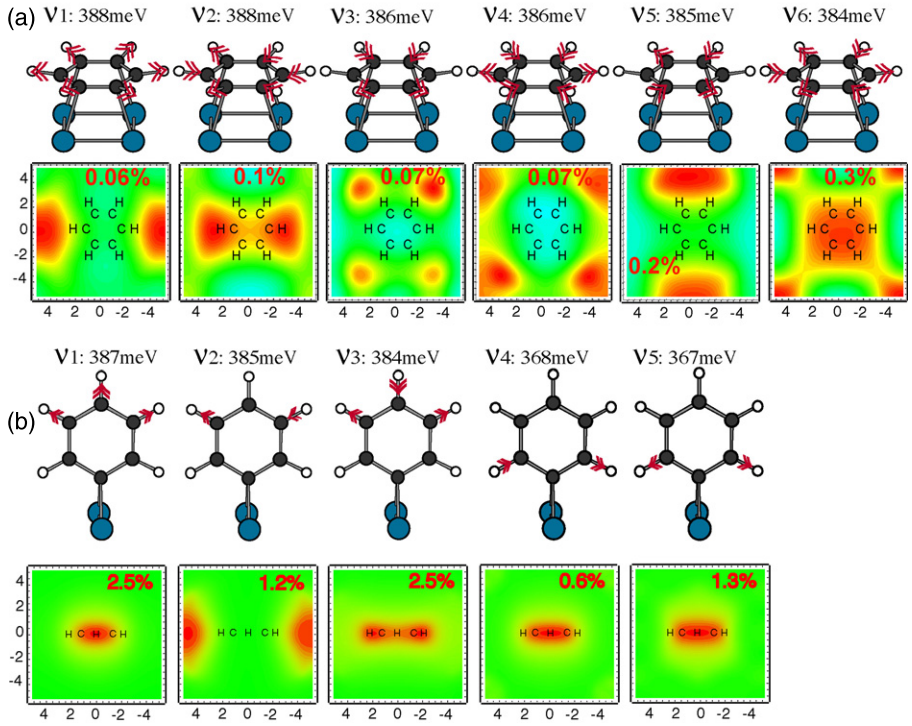

Figure 2. Spatial distribution of change in conductance due to the excitation of each C–H stretch mode of (a) benzene and (b) phenyl on Cu(100). The color scale goes from light blue (grey) to red (dark grey), minimum to maximum conductance change. The values of the maximum change are included on each panel.

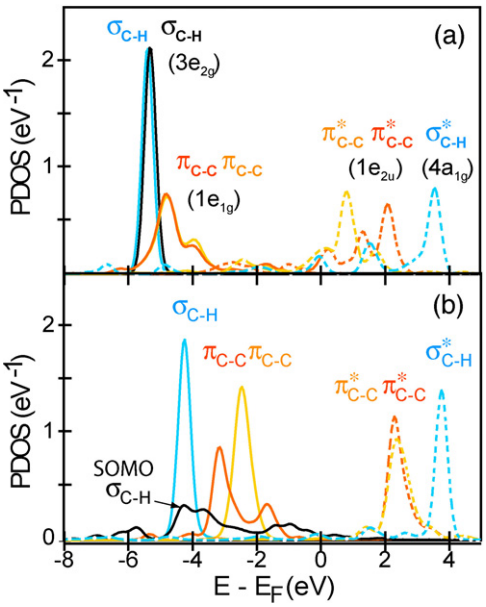

Figure 3. Projected density of states (PDOS) on substrate-free molecular orbitals for (a) benzene and (b) phenyl on Cu(100).

phenyl there is a distinct separation of the C–H stretch modes into two groups, leading to two resolvable peaks in the IETS spectra [12, 15].

The absence of IETS in the C–H stretch modes of benzene can be understood by analyzing the electronic structure of the benzene–copper system. Figure 3(a) shows the density of states projected onto the molecular orbitals of benzene [14, 26]; see equation (1). At the low bias voltages used for excitation of molecular modes, the electronic structure involved in the conduction process is the one at the Fermi energy. Figure 3(a) shows that the molecular character at the Fermi energy basically pertains to the π^* molecular orbitals; in other words, the electronic structure involves the ring structure. It is very difficult then to be able to excite the C–H stretch by injecting electrons into the π^* C–C electronic structure. Figure 3(b) shows the electronic structure in the presence of the phenyl fragment. In contrast to the benzene case, the PDOS at the Fermi energy presents a strong σ_{C-H} character. The tunneling electrons will have an important σ_{C-H} component with large C–H vibrational coupling.

3.2. *Pyridine reactions*

As revealed in the experimental data [15], pyridine presents some resemblances to benzene on Cu(100), but many differences due to its particular conformation on the surface. Figure 4 shows that pyridine sits on top of a Cu atom via its nitrogen dative bond [14]. In contrast, benzene lies flat on a hollow site. This has profound implications regarding the electronic structure and, hence, the interaction with the substrate and the reaction dynamics.

Figure 4 presents the adiabatic barriers and the reaction sequence for (a) rupture of the pyridine ring by the C–N bond and (b) dehydrogenation.

The ring disruption sequence leads to a final state in which the nitrogen atom lies on a hollow site and the carbon atom on a pseudo-bridge site. The ring is strained, but its strain is compensated by the high coordination of the broken ends with

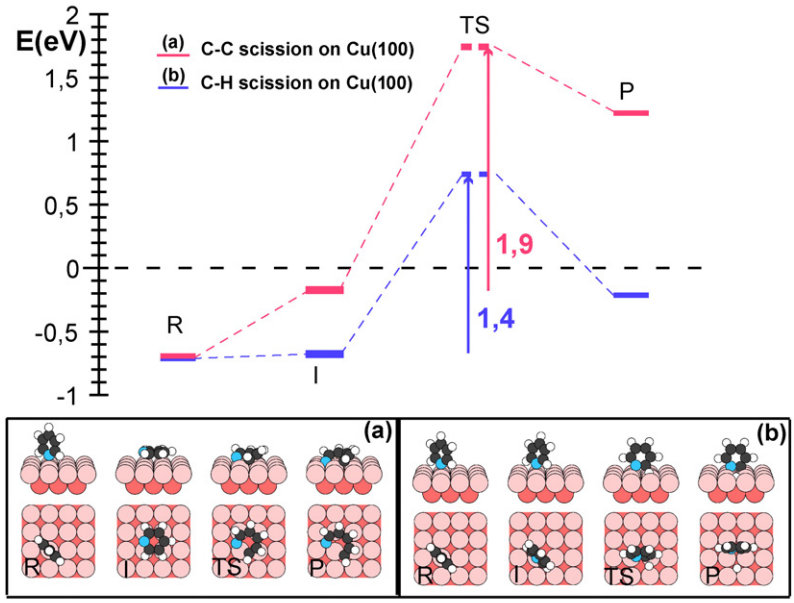

Figure 4. Adiabatic sequence for (a) ring disruption and (b) dehydrogenation of pyridine on Cu(100).

metallic atoms. The first stage of the reaction is to bend the upright molecule so as to increase the molecule's π^* orbital interaction with the metallic substrate. The consequence is charge transfer into the ring antibonding orbitals leading to the weakening of the C–N bonds. Next, the ring opens in a similar way to the ring rupture of the benzene molecule. The overall energy barrier is 2.4 eV, close to the 2.2 eV barrier found for the benzene case. Compared to dehydrogenation, the energy to sever the α-hydrogen is 1.4 eV, showing that energetically it is easier to dehydrogenate rather than to break the molecule's ring, as in the benzene case.

The sequence for dehydrogenation also involves some molecular conformation changes before bond breaking. First, the molecule has to rotate in order to increase the interaction of the α-hydrogen with the surface and to align the molecule with the surface row. The final stage is with the molecule on a hollow site, and the H atom lying on a next-neighbor hollow site. The scission by the α-hydrogen bond is facilitated by the weaker C–H bond of the α carbon atoms. This is due to the larger electronegativity of nitrogen that reduces the electronic charge of the nearby carbon atom.

3.2.1. Electronic structure of the reaction products. In order to understand both vibrational excitation and reactivity induced by tunneling electrons, it is instructive to study the electronic structure of the system in terms of the electronic structure of the molecular fragments. The presence of IETS signal for a given molecular mode can be traced back to a certain molecular character of the density of states at the Fermi energy [10, 11]. In the same way, the transfer of energy to a molecular system leading to a given molecular reaction has to be conveyed through the molecular electronic structure available at the particular bias voltage of the STM-induced reaction [14].

In [14], we found IETS signals for the C–H stretch mode of both pyridine and its dehydrogenated fragment. As we discussed there, the PDOS, figure 5, shows a clear density of states with (a) a HOMO and (b) singly occupied molecular orbital (SOMO) character at the Fermi energy. The corresponding molecular orbitals are depicted in figure 5. We find that the HOMO (SOMO) has an important weight on the σ_{C-H} of the molecule, qualitatively explaining why the electron-vibration coupling for the C–H stretch is sizable [14].

4. Discussion

The dehydrogenation reactions of benzene and pyridine entail a change in conformation in the first stages of the adiabatic pathway. Figure 1 shows that benzene must first desorb, while pyridine, figure 4, first rotates and plunges forward. This means that both reactions are initiated by the excitation of molecular motion as an external highly excited mode.

The excitation of this initial reaction coordinate involves electronic times in the subfemtosecond range, while the induced molecular motion is in the hundred femtosecond, even picosecond, scale. Hence, there are two well differentiated timescales: the electronic and the nuclear one. The reaction mechanism is reminiscent of the sudden vibrational excitation mechanism: the passing electron leaves the molecule in a mixed excited state caused by the short-lived appearance of an extra charge in the system. This is the opposite regime to a Franck–Condon process due to the transient of a negative ion (a recent example is given in [27]).

The electronic structure revealed in the PDOS, figures 3 and 5, is consistent with the sudden image. The electron will tunnel into the substrate via electronic states that have a molecular character associated with the molecule–surface bond. In the case of benzene, the π^* orbitals are largely responsible for the binding of the molecule to the surface [26]. It is in this electronic structure that the reacting electron is introduced, being efficiently coupled to the center-of-mass

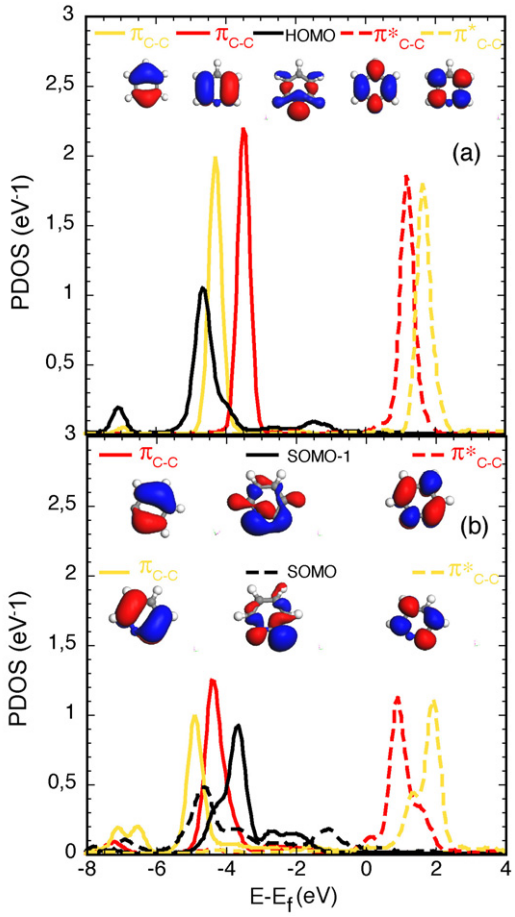

Figure 5. Projected density of states (PDOS) on substrate-free molecular orbitals for (a) pyridine and (b) its dehydrogenated fragment, C_5NH_4 on Cu(100).

motion of the molecule and easily inducing the first stages of the reaction. Similarly, in the case of pyridine, the HOMO is at the origin of the dative bond. Again, the HOMO-like electron structure is the prevailing molecular character at the Fermi energy, favoring molecular motion excitation.

After the initial electronic collision, the molecule remains largely neutral given the short lifetime of the electron in the molecular states. Subsequent electron injection can modify the evolution of the molecular system. In particular, a partially desorbed molecule will present larger lifetimes and will be prone to important inelastic effects by following tunneling electrons. However, this scenario does not occur. Experimentally, it has been determined that the dehydrogenation reactions are induced by a single electron [16].

Hence, the subsequent molecular evolution is going to be determined by the importance of non-adiabatic effects. These non-adiabatic effects will determine the rate of energy loss from the molecular degrees of freedom into the substrate ones. At high rates, all molecular dynamics will be quenched and reactions will be impossible. At low damping rates, non-adiabatic effects will be negligible and the reaction scenario proposed here (the adiabatic sequences of figures 1 and 4 for slowly moving molecular fragments) will be realistic. These adiabatic pathways have been computed under the assumption that no molecular electronic excitation takes place, which is a good approximation at low bias voltage. The experiments are performed at some 3 eV, probably in the limit where direct intramolecular electronic excitations can already take place.

At low voltages, the reactions will follow the adiabatic pathway in the case of the absence of non-adiabatic effects. Reference [28] shows that the damping rate due to substrate electronic excitations is inversely proportional to the molecular mass. The kinetic energy of the fragments is also inversely proportional to the square root of the masses of the fragments [29]. Hence, the heavier the molecular fragments, the more valid the adiabatic picture is.

The voltage threshold has been said to be unrelated to the energy barrier or to particular electronic resonances of the molecule–substrate system [16]. Our present results seem to confirm this statement. From the point of view of an adiabatic energy barrier, the voltage threshold has to account for the extra kinetic energy of the fragments as well as for sources of non-adiabatic processes, leading to damping and friction. Following the previous discussion, in the limit of large masses, one expects to retrieve the adiabatic evolution and hence the bias voltage will be directly connected with the energy barrier. This leads us to predict an isotope dependent behavior of the voltage threshold such that the threshold reduces as the isotope mass increases, opposite to what is found in [15]. Komeda and co-workers [16] have not found any isotope dependence of the bias voltage; however, the reaction yields are so small that it becomes increasingly difficult to determine the voltage threshold for heavier isotopes.

5. Conclusions

Density functional based calculations of benzene molecules chemisorbed on Cu(111), Cu(110) and Cu(100) and of pyridine on Cu(100) have been presented. The adiabatic reaction pathway for the molecular ring rupture of both molecules as well as of dehydrogenation has been evaluated. The energy barrier to break the molecular ring is found to be some 0.5 eV higher than the dehydrogenation barrier. This difference in energy is relatively small for the bias voltage applied in STM-induced reactions, leading us to the conclusion that rupture of the molecular rings is an open channel in the molecular reactions.

The binding energy is larger on the Cu(110) surface, given its more open geometry and hence more reactive surface structure, and it is lower for the more packed Cu(111) surface. The behavior is the opposite for the dehydrogenation energy barrier, being larger for the Cu(111) surface and smaller for the Cu(110) one. The reason behind this result is the larger charge transfer on the more reactive surface, Cu(110). On the more reactive surface, the antibonding molecular orbitals start having some minor population, enough to help the dissociation of the molecule.

The studied reactions always involve a conformational change of the molecule in the first stages of the reaction.

For benzene the molecule basically desorbs; for pyridine the molecule rotates and increases the H–surface interaction. These geometrical changes seem to be ubiquitous in the activation of STM-induced reactions.

The identification of the molecular fragments after the STM-induced reaction has been produced by comparing the IETS spectra with the simulated ones. A striking experimental finding is the absence of IETS signal in the C–H stretch modes of the chemisorbed benzene molecule. By computing the electronic structure and assigning the corresponding molecular character, we have been able to prove that only π^* orbitals are present at the Fermi energy of the substrate, rendering difficult the excitation of the C–H stretch modes because of the absent of direct couplings with this orbital. Along these lines, the excitation of the C–H stretch modes is possible in the different molecular fragments and pyridine because of the presence of electronic states with molecular σ_{C-H} character at the Fermi energy.

The studied reactions always entail the first excitation of extra molecular vibrational modes. These excitations lead to molecular conformational changes on the surfaces permitting the access to transition states along the reaction coordinates. The tunneling electronic residence lifetime in the molecule is in the subfemtosecond range, while these molecular motions skirt the picosecond timescale. Hence the excitation process is a sudden one: the electron passes, strongly perturbing the molecular system, that ends up relaxing in one of the reaction pathways. The actual reaction pathway will depend on the non-adiabatic effects involved in the molecular evolution. We have presented a discussion showing that isotopic effects will have their bearings on these non-adiabatic effects, since excitation lifetimes as well as the fragments' kinetic energies are considerably reduced with increasing fragment masses. Hence, the computed adiabatic barriers will match the measured voltage thresholds in the limit of heavy fragments.

Acknowledgments

Computational resources at IDRIS and CINES (CNRS) are gratefully acknowledged. Financial support has been obtained from the project ANR 'Jeunes Chercheurs' *INESS*. NL acknowledges support from the Spanish MEC (grant No FIS2006-12117-C04-01) and computer time from CESCA.

References

[1] Lee H J and Ho W 1999 *Science* **286** 1719
[2] Komeda T, Kim Y, Kawai M, Persson B N J and Ueba H 2002 *Science* **295** 2055
[3] Pascual J I, Lorente N, Song Z, Conrad H and Rust H-P 2003 *Nature* **423** 525
[4] Sloan P A and Palmer R E 2005 *Nature* **434** 367
[5] Stipe B C, Rezaei M A and Ho W 1998 *Science* **280** 1732
[6] Lauhon L J and Ho W 2000 *Phys. Rev. Lett.* **84** 1527
[7] Lauhon L J and Ho W 2001 *Rev. Sci. Instrum.* A **72** 216
[8] Kim Y, Komeda T and Kawai M 2002 *Phys. Rev. Lett.* **89** 126104
[9] Lorente N and Persson M 2000 *Phys. Rev. Lett.* **85** 2997
[10] Lorente N, Persson M, Lauhon L J and Ho W 2001 *Phys. Rev. Lett.* **86** 2593
[11] Lorente N, Rurali R and Tang H 2005 *J. Phys.: Condens. Matter* **17** S1049
[12] Bocquet M-L, Lesnard H and Lorente N 2006 *Phys. Rev. Lett.* **96** 096101
[13] Bocquet M-L and Loffreda D 2005 *J. Am. Chem. Soc.* **127** 17207
[14] Lesnard H, Bocquet M-L and Lorente N 2007 *J. Am. Chem. Soc.* **129** 4298
[15] Lauhon L J and Ho W 2000 *J. Phys. Chem.* A **104** 2463
[16] Komeda T, Kim Y, Sainoo Y and Kawai M 2004 *J. Chem. Phys.* **120** 5347
[17] Kresse G and Fürthmuller J 1996 *Comput. Mater. Sci.* **6** 15
[18] Kresse G and Joubert D 1999 *Phys. Rev.* B **59** 1758
[19] Henkelman G, Uberuaga B and Jonsson H 2000 *J. Chem. Phys.* **113** 9901
[20] Tersoff J and Hamman D R 1983 *Phys. Rev. Lett.* **50** 1998
[21] Lomas J R and Pacchioni G 1996 *Surf. Sci.* **365** 297
[22] Triguero L, Pettersson L G M, Minaev B and Agren H 1998 *J. Chem. Phys.* **108** 3
[23] Xi M, Yang M X, Jo S K, Bent B E and Stevens P 1994 *J. Chem. Phys.* **101** 9122
[24] Lukes S, Vollmex S, Witte G and Wöll G 2001 *J. Chem. Phys.* **114** 10123
[25] Lomas J R, Baddeley C J, Tikhov M S and Lambert R M 1995 *Langmuir* **11** 3048
[26] Lorente N, Hedouin M F G, Palmer R E and Persson M 2003 *Phys. Rev.* B **68** 155401
[27] Berthe M *et al* 2006 *Phys. Rev. Lett.* **97** 206801
[28] Hellsing B and Persson M 1984 *Phys. Scr.* **29** 360
[29] Gadzuk J W 1995 *Surf. Sci.* **342** 345